RSC Advances

PAPER

View Article Online
View Journal | View Issue

Cite this: *RSC Adv.*, 2025, **15**, 39305

Eco-friendly synthesis of ZnO nanoparticles using *Delonix elata* extract with enhanced antibacterial activity

Jayashree Nanthakumar,[a] Yasotha Palanisamy,*[a] Sivasubramanian Palanisamy,*[b] Manickaraj Karuppusamy,[c] Ramkumar Raja,[de] Mohamed Abbas,[de] Aravindhan Alagarsamy[f] and Md Zillur Rahman*[g]

In this study, zinc oxide (ZnO) nanoparticles (NPs) were successfully synthesized using a green and eco-friendly method employing the aqueous leaf extract of *Delonix elata* as a natural reducing and stabilizing agent. Characterization of the synthesized nanoparticles was performed using a range of techniques, including X-ray diffraction (XRD), Fourier-transform infrared (FTIR) spectroscopy, ultraviolet-visible (UV-Vis) spectroscopy, scanning electron microscopy (SEM), energy-dispersive X-ray (EDX) spectroscopy, high-resolution transmission electron microscopy (HR-TEM), and selected area electron diffraction (SAED). XRD analysis revealed the formation of a hexagonal wurtzite structure with an average crystallite size of 30.1 nm. FTIR spectra confirmed the involvement of phytochemicals in the stabilization process. UV-Vis spectroscopy showed an absorption peak at 311 nm, corresponding to an optical band gap of 2.7 eV. SEM and HR-TEM images demonstrated predominantly spherical NPs with a well-defined morphology. The antibacterial activity of the ZnO NPs was evaluated against both Gram-positive *Staphylococcus aureus* and Gram-negative *Escherichia coli* strains. The results revealed significant inhibition against *E. coli*, with no inhibition observed for *S. aureus*. These findings suggest that green-synthesized ZnO NPs possess strong antibacterial potential, particularly against Gram-negative bacteria, and offer a sustainable and cost-effective alternative to conventional methods for NP synthesis in biomedical applications.

Received 19th July 2025
Accepted 6th October 2025

DOI: 10.1039/d5ra05208d

rsc.li/rsc-advances

1 Introduction

Microbial infections continue to pose a significant threat to human health and environmental safety. Historically, pathogenic bacteria, fungi, and viruses have been the primary causes of infectious diseases. Since Fleming discovered penicillin in 1928, numerous antibiotics have been developed.[1] Due to their strong bactericidal activity and relatively low toxicity to mammalian cells, antibiotics have long been regarded as the primary method of infection management. Without them, even basic medical procedures would be challenging to perform. However, the widespread misuse and overuse of antibiotics have accelerated the emergence of multidrug-resistant strains, posing a severe global health challenge.[2] The pace of antimicrobial drug discovery has not kept pace with the rapid evolution of resistance, fueling concerns about an impending "post-antibiotic era".[3] It is estimated that drug-resistant infections currently cause 700 000 deaths annually, a figure projected to rise to 10 million by 2050, with an associated economic burden of more than $100 trillion. Despite the urgent need for new antibacterial agents, high development costs, lengthy timelines, and limited financial returns have led pharmaceutical companies to reduce their investment in antibiotic discovery.[4]

Nanotechnology offers an alternative strategy for addressing antimicrobial resistance. Broadly defined, it encompasses the manipulation and application of matter at the nanoscale (1–100 nm), where materials exhibit unique chemical, physical, and biological properties.[5–9] Nanostructured systems have already shown promise in biomedical, electronic, and environmental applications due to their enhanced functionality compared to their bulk counterparts. Among nanomaterials, zinc oxide (ZnO) has been studied extensively since the early 20th century.

[a]*Department of Physics, Navarasam Arts and Science College for Women, Arachalur, Erode, Tamilnadu, India. E-mail: yasothap238@gmail.com*

[b]*Department of Mechanical Engineering, P T R College of Engineering & Technology, Thanapandian Nagar, Madurai – Tirumangalam Road, Madurai, 625008, Tamilnadu, India. E-mail: sivaresearch948@gmail.com*

[c]*Department of Mechanical Engineering, CMS College of Engineering and Technology, Coimbatore 641032, Tamil Nadu, India*

[d]*Central Labs, King Khalid University, P. O. Box 960, AlQura'a, Abha, Saudi Arabia*

[e]*Electrical Engineering Department, College of Engineering, King Khalid University, Abha 61421, Saudi Arabia*

[f]*Department of Electronics and Communication Engineering, Koneru Lakshmaiah Education Foundation, Vaddeswaram, Andhra Pradesh, 522501, India*

[g]*Department of Mechanical Engineering, Ahsanullah University of Science and Technology, Dhaka 1208, Bangladesh. E-mail: md.zillur.rahman.phd@gmail.com*

Following the advent of the semiconductor era, ZnO gained attention for its electronic and optoelectronic properties, including piezoelectricity, diluted ferromagnetism, and excitonic behavior.[10–13] Its high exciton binding energy (60 meV), exceeding the thermal energy at room temperature (26 meV), makes it particularly suitable for exciton-based devices.[14,15] In addition, ZnO nanostructures exhibit significant antibacterial, antifungal, and photocatalytic activities, supporting their application in healthcare, food safety, and water purification.

Conventional physical and chemical methods for synthesizing ZnO nanoparticles (ZnO NPs), including sol–gel processing, chemical vapor deposition, and plasma arcing, often require high energy input and toxic reagents, generating hazardous by-products.[16,17] In contrast, green synthesis using biological resources offers an eco-friendly, cost-effective, and energy-efficient alternative.[18,19] Plant-mediated synthesis, in particular, is attractive because phytochemicals act simultaneously as reducing and stabilizing agents, enabling rapid NP formation under ambient conditions.[20,21]

Delonix elata Linn. (family: Caesalpinaceae) is a deciduous tree native to the dry forests of India. Its leaves' and bark's extracts are traditionally used in Karnataka for treating jaundice, hepatic disorders, bronchial ailments, and rheumatism.[11,12] Previous studies have reported its antinociceptive,[13] antibacterial,[16] and anti-inflammatory[22] properties. These biological activities are attributed to its rich phytochemical profile, including flavonoids, phenolics, tannins, and terpenoids. Therefore, the present study uniquely explores the green synthesis of ZnO NPs using *D. elata* leaf extract as a natural reducing and stabilizing agent. This approach minimizes toxic by-products, lowers production costs, and enhances the biocompatibility of the nanomaterials. The phytoconstituents of *D. elata* not only facilitate NP synthesis and stabilization but may also impart additional antioxidant and therapeutic properties to the nanocomposites. Importantly, scalable biosynthesis of ZnO NPs using locally available plant resources can provide sustainable antibacterial materials for healthcare textiles, food-contact surfaces, and water-treatment coatings, particularly in resource-limited settings. From a societal perspective, this scalable green synthesis reduces the need for hazardous reagents and energy consumption, supporting the development of safer and more environmentally friendly antibacterial materials.

2 Experimental details

2.1 Materials

Zinc acetate (99%, analytical grade) was procured from Scientific and Chemicals, Erode, Tamil Nadu, India, and used as received without further purification. Fresh leaves of *Delonix elata* Linn. were collected from mature trees located in Erode, Tamil Nadu, India.

2.2 Preparation of leaf extract

Fresh *Delonix elata* leaves were thoroughly washed with tap water to remove surface dust and other impurities, followed by rinsing with deionized water. The cleaned leaves were then air-dried at room temperature. Approximately 30 g of the dried leaves was mixed with 100 mL of deionized water and subjected to microwave-assisted extraction at 70 W under continuous stirring. A noticeable color change in the solution indicated the successful extraction of phytochemicals. The mixture was subsequently cooled to room temperature and filtered through Whatman no. 1 filter paper to obtain a clear filtrate. The resulting extract was stored at 4 °C for further use in the synthesis of ZnO NPs.

2.3 Synthesis of leaf-capped zinc oxide

ZnO NPs were synthesized using *Delonix elata* leaf extract as a natural reducing and stabilizing agent. In a typical procedure, 2 g of zinc acetate was dissolved in 50 mL of distilled water. To this solution, 20 mL of freshly prepared *Delonix elata* leaf extract was added under continuous stirring for 30 minutes.[23,24] Subsequently, 30 mL of 0.5 M NaOH solution was introduced dropwise while maintaining a constant pH of 12. A gradual color change from green to pale yellow indicated the nucleation of ZnO NPs. The reaction mixture was then left undisturbed for 24 hours to ensure complete precipitation. The resulting precipitate was collected, thoroughly washed with distilled water to remove impurities, and dried in a microwave oven at 70 W for 1 hour.[25] To improve crystallinity, the dried product was calcined in a muffle furnace at 400 °C for 4 hours under controlled conditions. The final ZnO NPs, capped with phytochemicals from the leaf extract, were finely ground into a uniform powder using a mortar and pestle.

3 Results and discussion

3.1 Ultra violet visible spectroscopy(UV-Vis)

Fig. 1a depicts the absorption spectrum of ZnO NPs recorded in the ultraviolet–visible (UV-Vis) spectral region. The ZnO sample exhibits a clear absorption band at 311 nm, confirming the successful fabrication of ZnO NPs.[26,27] The optical band gap (E_g) was calculated from the absorption data using the Tauc relation (eqn (1)).

$$\alpha E_p = K(E_p - E_g)^{1/2} \quad (1)$$

where α is the absorption coefficient, E_p is the photon energy, E_g is the optical band gap, and K is the material-dependent constant. As shown in Fig. 1b, a Tauc plot was generated by plotting $(\alpha E_p)^2$ against E_p to calculate E_g. By extending the graph's linear segment to the energy axis at $\alpha = 0$, the optical band gap of ZnO NPs was determined.[28–31] The empirically measured band gap value is 2.7 eV, which is in agreement with values in earlier literature.[26,32–34]

3.2 Functional group analysis

Fourier transform infrared (FTIR) spectroscopy is a crucial analytical technique for identifying functional groups, molecular shape, and intramolecular and intermolecular interactions in a chemical compound. The FTIR spectrophotometer

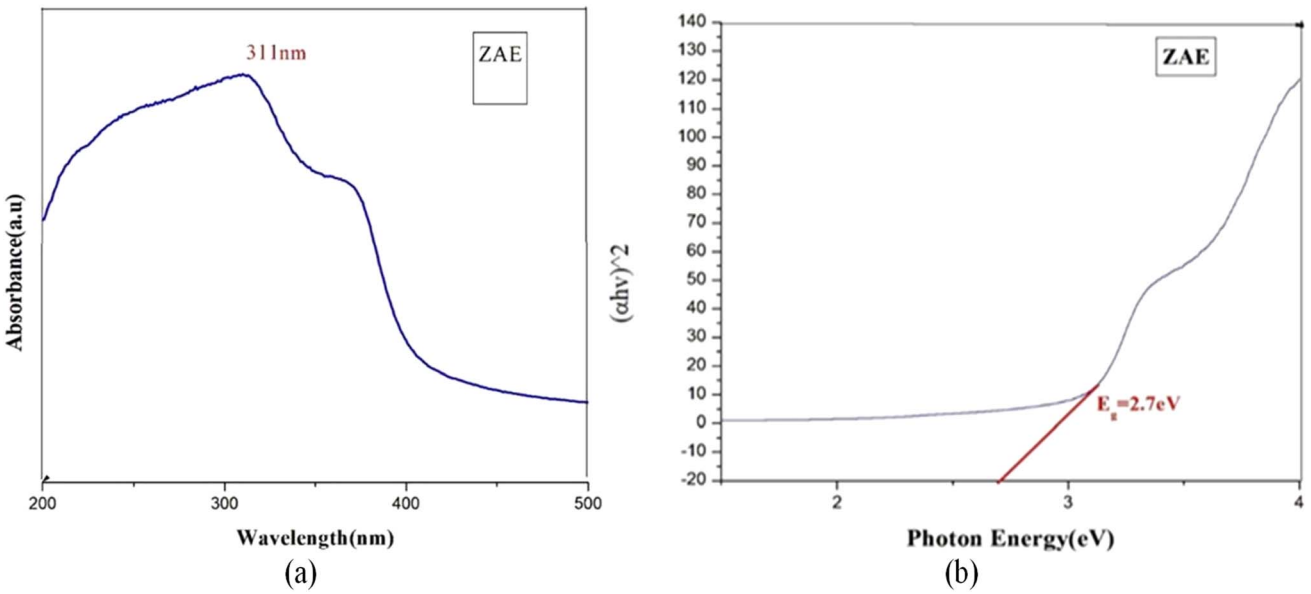

Fig. 1 (a) UV-Vis absorption spectrum of ZnO NPs synthesized using *Delonix elata* leaf extract (absorption peak at 311 nm) and (b) Tauc plot for estimating the optical band gap of ZnO NPs synthesized using *Delonix elata* leaf extract ($E_g = 2.7$ eV).

measures the infrared absorbance or transmittance of a substance depending on its wavenumber by forming distinct absorption bands that correspond to certain functional groups.[35–37] Fig. 2 shows the FTIR spectrum of ZnO NPs produced using a green synthesis approach that includes leaf extract from *Delonix elata*. The spectra were acquired within the 4000–400 cm^{-1} range.[38–40] The absorption peaks in the spectrum demonstrate the presence of several functional groups involved in NP reduction and stability. The presence of alcohol or phenolic chemicals in the plant extract is suggested by a prominent absorption band at about 3600 cm^{-1}, which is indicative of O–H stretching vibrations related to hydroxyl groups.[41–44] The signal at 3266 cm^{-1} results from stretching of the hydroxyl (O–H) groups. The peak at 2984 cm^{-1} is caused by C–H stretching vibrations, perhaps from methine or methylene groups. Additional absorption bands at 2332, 1526, and 954 cm^{-1} indicate the existence of amine or ammonia functional groups, corresponding to N–H stretching and bending modes. C–H bending and C–CHO (aldehyde) stretching vibrations have absorption maxima at 1406 cm^{-1} and 1051 cm^{-1},

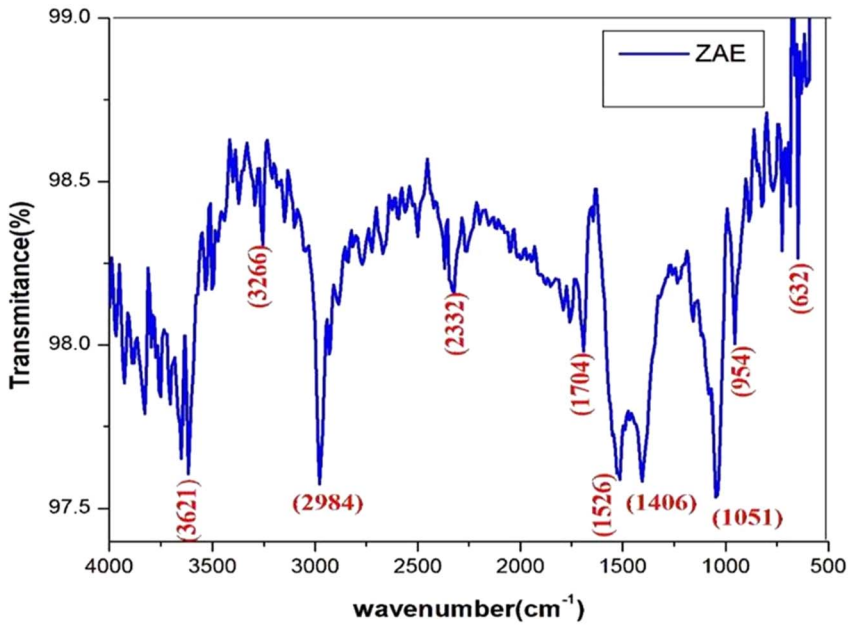

Fig. 2 FTIR spectrum of ZnO NPs synthesized using *Delonix elata* leaf extract.

Table 1 XRD parameters of ZnO NPs synthesized using Z. *elata* extract (ZAE)

Sample	2θ (°)	d (Å)	FWHM (°)	hkl	$a = b$ (Å)	c (Å)	Crystallite size D (nm)	Unit cell volume V (Å^3)	Dislocation density δ ($\times 10^{15}$ m^{-2})	Microstrain ε
ZAE	36.1742	2.48113	0.2881	101	3.25	5.24	29.8	47.93	112.269	0.2218
	47.4498	1.91452	0.3034	102	3.25	5.20	28.9	47.56	119.730	0.2338
	62.7595	1.47933	0.3235	103	3.20	5.28	29.0	63.85	118.906	0.1585
	67.8484	1.38023	0.3463	112	3.25	5.18	28.1	47.38	126.644	0.1454
	76.8377	1.23961	0.3244	202	3.22	5.22	31.6	46.11	100.144	0.1300
	81.2754	1.18276	0.3106	104	3.24	5.20	33.7	46.12	88.0521	0.1585
	89.4932	1.09422	0.3872	203	3.23	5.21	29.4	46.20	115.692	0.1339
Average	—	—	—	—	3.23	5.22	30.1	49.31	111.63	0.169

respectively. The cyanate group may have a potential impact on the bands in this area.[45,46] The distinctive peaks show that bioactive chemicals from *Delonix elata* leaf extract contributed to the formation and stabilisation of ZnO NPs.[47,48]

3.3 X-ray diffraction analysis (XRD)

XRD analysis was performed to evaluate the crystallographic structure, crystallite size, and crystallinity of the synthesized ZnO NPs, with the corresponding values presented in Table 1. The XRD pattern (Fig. 3) displayed distinct Bragg reflections at 2θ values of 36.14° (101), 47.44° (102), 62.75° (103), 67.84° (112), 76.83° (202), 81.27° (104), and 89.49° (203). A total of seven diffraction peaks were indexed to the hexagonal wurtzite ZnO structure (space group $P6_3mc$, $a = 3.2$ Å, $c = 5.20$ Å), matching the standard JCPDS card no. 36-1451 ref. 49 and confirming the phase purity. The most intense diffraction peak, observed at 36° and corresponding to the (101) plane, is in agreement with earlier studies.[50–53] The sharper, more intense reflections observed for the ZnO NPs, compared to those of the zinc Schiff base precursor, indicate superior crystallinity. No secondary or impurity peaks were detected, further confirming the successful formation of pure ZnO NPs.[54] The average crystallite size, calculated using the Debye–Scherrer equation ($D = 0.891\lambda/\beta\cos\theta$) based on the full width at half maximum of the (101) peak, was approximately 30.1 nm, consistent with SEM observations. The narrow peak broadening also suggests that the ZnO NPs are well-crystallized with a size below 50 nm.[55,56]

3.4 Scanning electron microscope (SEM)

The leaf extract of *Delonix elata* has a significant impact on the shape of the resultant ZnO structures, as evident in SEM images (Fig. 4a–c) of the synthesized ZnO NPs produced by the green synthesis technique. The synthesized ZnO exhibits an average primary particle size of around 200 nm and is primarily composed of NPs and nanoflower-like structures. The tendency of the initial NPs to coalesce resulted in the formation of larger secondary agglomerates.[57,58] Fig. 4b illustrate that using a higher concentration of *Delonix elata* leaf extract resulted in denser and smoother ZnO NPs. The particle thickness varied from 8 to 30 nm, with an average lateral dimension of around 200 nm.[59–62] SEM scans revealed densely packed, erratically aligned, and overlapping ZnO nanostructures, with most

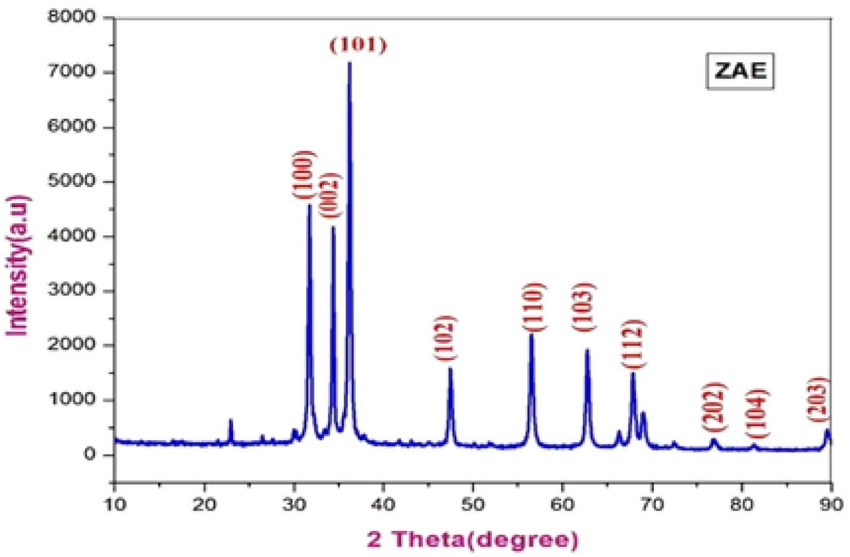

Fig. 3 XRD diffraction pattern of ZnO NPs synthesized using *Delonix elata* leaf extract.

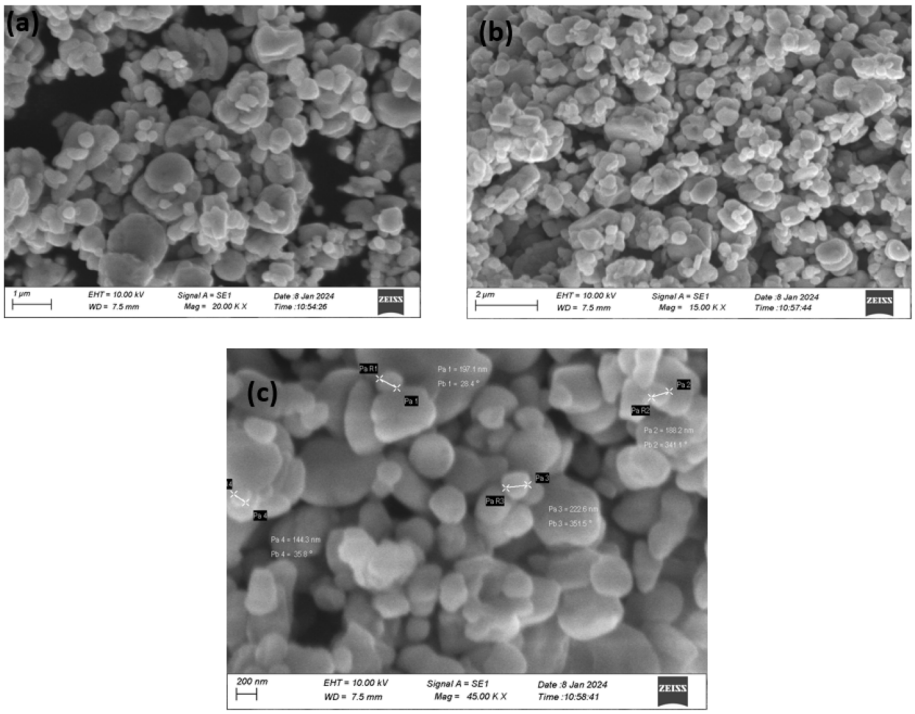

Fig. 4 SEM micrographs of ZnO NPs synthesized using *Delonix elata leaf* extract.

particles having lateral diameters smaller than 1 μm. Consistent with the XRD data, the shape and particle distribution displayed in the SEM micrographs confirm the high crystallinity and near-perfect stoichiometry of the synthesised ZnO NPs.[63,64]

3.5 HR-TEM and SAED analysis

The morphological and structural features of the bio-osynthesized ZnO NPs were further investigated using high-resolution transmission electron microscopy (HR-TEM) and selected area electron diffraction (SAED). The HR-TEM micrographs (Fig. 5a and b) demonstrate that the ZnO NPs synthesized with *Delonix elata* leaf extract predominantly exhibit spherical to quasi-spherical morphologies, with a tendency to agglomerate into clusters. The particle boundaries are well-defined, and the average particle size falls within the nanometer range, confirming the stabilization effect of the phytochemicals in the plant extract.[65] The observed agglomeration is consistent

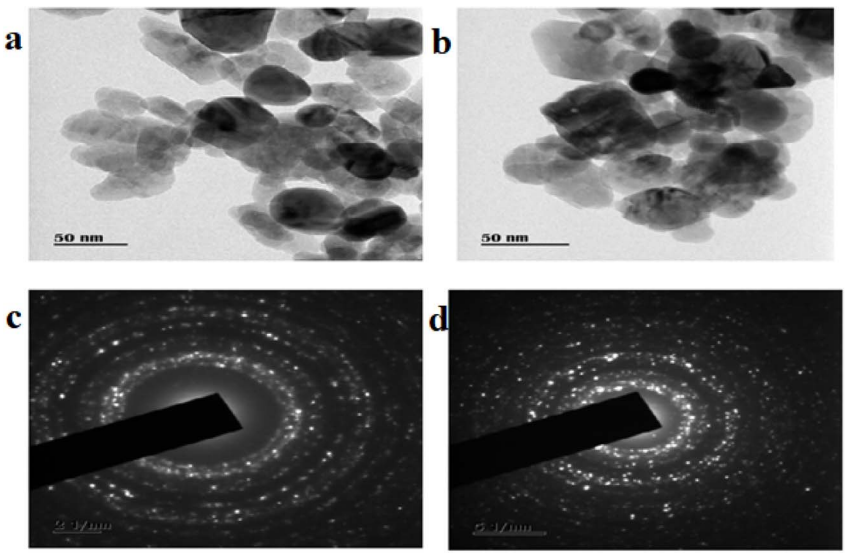

Fig. 5 (a and b) HR-TEM images of ZnO NPs synthesized using *Delonix elata* leaf extract, and (c and d) SAED patterns confirming their crystalline nature.

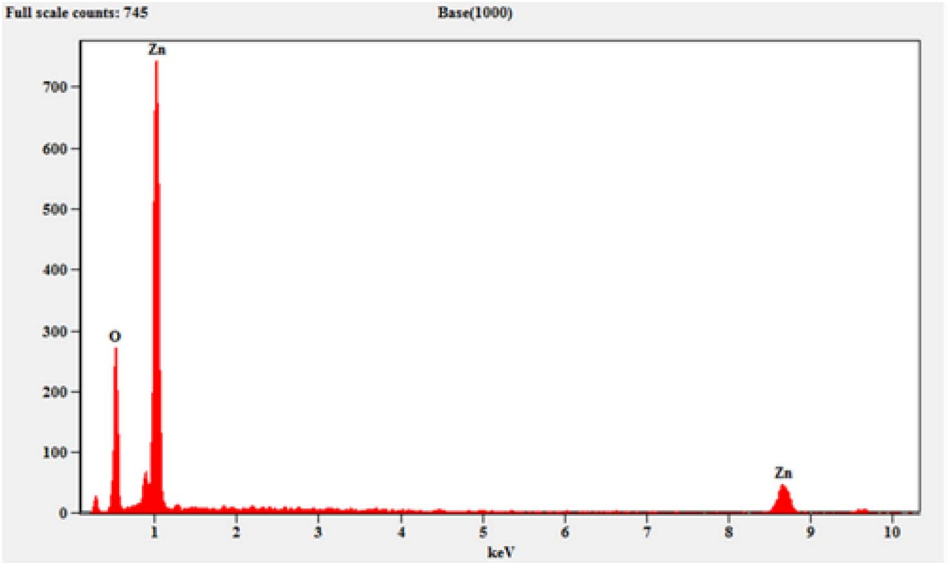

Fig. 6 EDX analysis of ZnO NPs using *Delonix elata* leaves extract.

Table 2 Elemental composition and atomic/weight percentages of ZnO NPs

Element line	Weight (%)	Weight error (%)	Atom (%)
OK	32.54	0.98	66.35
ZnK	67.46	4.64	33.65
ZnL	—	—	—
Total	100.00		100.00

with the high surface energy and strong van der Waals forces typical of nanoscale materials. The SAED patterns (Fig. 5c and d) exhibit sharp concentric diffraction rings with bright spots, indicating the polycrystalline nature of the ZnO NPs.[62,66] These rings correspond to the (100), (002), (101), (102), (110), and (103) crystal planes of the hexagonal wurtzite phase of ZnO, which aligns with XRD findings. The clarity and continuity of the rings reflect a high degree of crystallinity, crucial for optimizing the optical and biological properties of ZnO NPs. These results confirm that the green synthesis method using *Delonix elata* leaf extract not only facilitates NP formation but also enhances their stability and crystallinity. Such features highlight the potential of this eco-friendly approach for producing ZnO NPs suitable for various biomedical and environmental applications.[67,68]

3.6 Energy dispersive X-ray spectroscopy (EDX)

EDX was employed to assess the synthesised NPs both qualitatively and quantitatively, and to determine their elemental composition.[69–72] Fig. 6 shows the EDX spectrum of ZnO NPs, while Table 2 lists the key elements identified. The analysis revealed the presence of essential elements, including zinc (Zn) and oxygen (O), alongside their respective atomic and weight percentages in the samples. The results indicate a high degree of purity in the synthesized NPs, underscoring the role of bioactive compounds from the plant extract in NP formation.[73,74] Additionally, the EDX analysis showed no detectable impurities or extraneous free radicals, confirming the effectiveness and purity of the synthesis method.

3.7 Antibacterial activity

The antibacterial activity of the synthesized ZnO NPs prepared using *Delonix elata* leaf extract was assessed against both Gram-positive *Staphylococcus aureus* and Gram-negative *Escherichia coli* strains using the agar well diffusion method, as presented in Table 3. Fig. 7a and b illustrate the inhibition zones observed at various concentrations (100 μg mL^{-1}, 250 μg mL^{-1}, and 500 μg mL^{-1}) of ZnO NPs, with the negative control (NC) showing no inhibitory effect.[75–77] In *S. aureus* (Fig. 7a), no concentration resulted in the largest zone of inhibition, indicating a strong antibacterial effect.[76–78] The inhibitory effect decreased at lower

Table 3 Zone of inhibition (mm) of *Z. elata* extract (ZAE) against *Staphylococcus aureus* and *Escherichia coli* (mean ± SD)

Test organism	Test sample	500 μg mL^{-1}	250 μg mL^{-1}	100 μg mL^{-1}	50 μg mL^{-1}	PC (positive control)
Staphylococcus aureus	ZAE	0	0	0	0	16.75 ± 1.06
Escherichia coli	ZAE	6.5 ± 0.71	0	0	0	14.5 ± 0.71

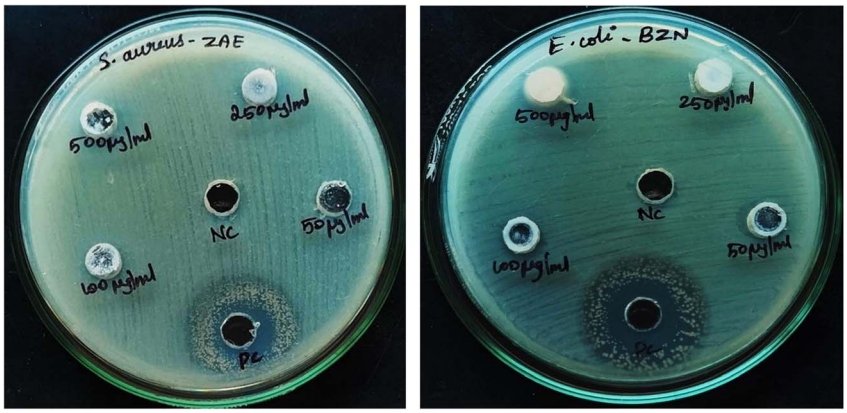

Fig. 7 (a) Antibacterial activity of ZnO NPs synthesized using *Delonix elata leaf* extract: (a) Gram-positive *Staphylococcus aureus* and (b) Gram-negative *Escherichia coli*.

concentrations, demonstrating a clear dose-dependent response. Similarly, in *E. coli* (Fig. 7b), ZnO NPs exhibited significant inhibition at higher concentrations, confirming their activity against Gram-negative bacteria. These results suggest that the biosynthesized ZnO NPs possess broad-spectrum antibacterial potential, likely due to their ability to generate reactive oxygen species (ROS) and disrupt bacterial cell membranes. The enhanced antibacterial activity may also stem from the synergistic effect of bioactive phytochemicals in *Delonix elata* extract, which likely assisted in capping and stabilizing the NPs while retaining some intrinsic antibacterial properties.[79]

3.8 Statistical analysis

The optical band gap determined from UV-Vis spectroscopy was consistent at 2.7 eV across replicates, with negligible variation, confirming reproducibility. FTIR spectra reproducibly displayed characteristic O–H, C–H, N–H, and C═O bands, indicating stable involvement of phytochemicals without significant variation in peak occurrence. XRD analysis across seven crystallographic planes yielded an average crystallite size of 30.1 ± 0.19 nm, with one-way ANOVA confirming no statistically substantial variation between planes ($p > 0.3$). Microstrain (0.169 ± 0.042) and dislocation density (111.6 ± 13.2 × 10^{15} m^{-2}) showed moderate variation, while unit cell volumes were largely uniform except for a single outlier plane. TEM and SAED analyses qualitatively confirmed spherical morphology and polycrystalline wurtzite structure, consistent with XRD findings. EDX measurements revealed Zn and O as the sole constituents, with mean atomic fractions of 33.7% Zn and 66.3% O. A chi-square test against ideal 1 : 1 stoichiometry indicated a statistically significant deviation ($p < 0.01$), suggesting an O-rich surface composition. Antibacterial assays (triplicates, mean ± SD) demonstrated no inhibition of *Staphylococcus aureus* at any concentration tested, while *Escherichia coli* exhibited significant inhibition at 500 μg mL^{-1} (6.5 ± 0.7 mm). One-way ANOVA confirmed a strong concentration-dependent effect for *Escherichia coli* ($F \approx 3169$, p ″0.001), with post hoc analysis indicating the highest dose was significantly different from all lower concentrations ($p < 0.01$). Overall, statistical evaluation confirmed uniform nanocrystalline structure, significant deviation in Zn : O stoichiometry, and dose-dependent antibacterial activity selectively against Gram-negative bacteria.

4 Conclusion

The green synthesis of ZnO NPs using *Delonix elata* leaf extract presents a promising, eco-friendly, and cost-effective approach for producing NPs with notable antibacterial potential. Characterization analyses confirmed the successful formation of ZnO NPs exhibiting a well-defined hexagonal wurtzite structure, an average crystallite size of approximately 30.1 nm, and enhanced optical properties with a band gap of 2.7 eV. The phytochemicals present in the plant extract played vital roles in the reduction, nucleation, and stabilization of the NPs, highlighting the effectiveness of bioactive compounds in green synthesis. Antibacterial evaluation demonstrated significant inhibition against *Escherichia coli*, whereas no activity was observed against *Staphylococcus aureus*, indicating the selective antibacterial efficacy of the synthesized ZnO NPs. This selectivity highlights their potential for targeting specific bacterial strains while revealing limitations in their broad-spectrum applicability. Additional limitations of this study include the restricted range of bacterial strains tested, the absence of mechanistic insights into bacterial inhibition, and the lack of cytotoxicity or *in vivo* biocompatibility assessments, all of which are crucial for clinical translation. Future research may expand antibacterial testing to include multiple Gram-positive and Gram-negative strains, including drug-resistant pathogens, and elucidate the underlying inhibition mechanisms, such as ROS generation or membrane disruption. Moreover, further studies can also focus on cytotoxicity assessments, *in vivo* biocompatibility, and optimization of scalable synthesis protocols while evaluating environmental impacts. Addressing these aspects will enhance the practical applicability of *Delonix elata*-derived ZnO NPs, facilitating their integration into antimicrobial

coatings, wound healing, infection control, and other sustainable biomedical applications.

Author contributions

Jayashree Nanthakumar: performed data collection, conducted experiments, and prepared the initial draft; Yasotha Palanisamy: conceived the study, designed methodology, supervised the project, and contributed to manuscript editing; Sivasubramanian Palanisamy: co-supervised the research, assisted in conceptualization, and critically reviewed and revised the manuscript; Manickaraj Karuppusamy: assisted with data analysis, validation, and visualization; Ramkumar Raja: contributed resources, supported experimental setup, and managed project administration; Mohamed Abbas: assisted in data curation, formal analysis, and manuscript review; Aravindhan Alagarsamy: contributed to refinement of methodology and interpretation of results; Md Zillur Rahman: provided overall supervision, contributed to critical revision, reviewed and edited the manuscript, and finalized the manuscript for publication.

Conflicts of interest

The authors declared no potential conflicts of interest with respect to the research, authorship, and/or publication of this article.

Data availability

Data are available on request from the authors.

Acknowledgements

The authors extend their appreciation to University Higher Education Fund for funding this research work under Research Support Program for Central labs at King Khalid University through the project number CL/CO/A/4.

References

1 G. A. Mansoori and T. A. F. Soelaiman, *Nanotechnology–An Introduction for the Standards Community*, ASTM International, Chicago, IL, USA, 2005.
2 L. E. Lwakatare, A. Raj, I. Crnkovic, J. Bosch and H. H. Olsson, *Inf. Software Technol.*, 2020, **127**, 106368.
3 V. Balamurugan, C. Ragavendran, D. Arulbalachandran, A. F. Alrefaei and R. Rajendran, *Inorganic Chemistry Communications*, 2024, **168**, 112882.
4 J. Cai and R. Liu, *Biomater. Sci.*, 2020, **8**, 6812–6813.
5 T. Kaehler, *Clin. Chem.*, 1994, **40**, 1797.
6 M.-C. Daniel and D. Astruc, *Chem. Rev.*, 2004, **104**, 293–346.
7 C. N. R. Rao and A. K. Cheetham, *J. Mater. Chem.*, 2001, **11**, 2887–2894.
8 C. Merzbacher, in *Women in Nanotechnology: Contributions from the Atomic Level and up*, Springer, 2019, pp. 121–133.
9 M. R. Miloud, in *SHS Web of Conferences*, EDP Sciences, 2023, vol. 172, p. 3012.
10 G. Parthasarathy, M. Saroja, M. Venkatachalam, S. Shankar and V. K. Evanjelene, *World J. Pharm. Pharmaceut. Sci.*, 2016, **5**, 922–931.
11 C. Wijayasiriwardena, P. P. Sharma, M. G. Chauhan and A. P. G. Pillai, *Int. J. Res. Ayurveda Pharm.*, 2009, **30**, 68–72.
12 P. S. Pavithra, V. S. Janani, K. H. Charumathi, R. Indumathy and S. V. Rama, *Int. J. Green Pharm.*, 2010, 22–28.
13 K. Pradeepa, K. Venkatarangaiah, B. G. Harish, R. Venkatesh, S. K. SR and G. Kumar, *J. Biochem. Technol.*, 2014, **3**, 193–197.
14 K. Ellmer and A. Klein, in *Transparent Conductive Zinc Oxide: Basics and Applications in Thin Film Solar Cells*, Springer, 2008, pp. 1–33.
15 S. Rokkarukala, T. Cherian, C. Ragavendran, R. Mohanraju, C. Kamaraj, Y. Almoshari, A. Albariqi, M. H. Sultan, A. Alsalhi and S. Mohan, *Heliyon*, 2023, e14668.
16 K. Pradeepa, V. Krishna, K. K. Girish, S. Kumar SR, J. H. Hoskeri and A. U. Gnanesh, *Asian Pac. J. Trop. Biomed.*, 2012, **2**, S229–S231.
17 P. Krishnappa, K. Venkatarangaiah, Venkatesh, S. K. Shivamogga Rajanna and R. Kashi Prakash Gupta, *BioMed Res. Int.*, 2014, **2014**, 507851.
18 K. Parveen, V. Banse and L. Ledwani, in *AIP Conference Proceedings*, AIP Publishing LLC, 2016, vol. 172420048.
19 J. Xu, Y. Huang, S. Zhu, N. Abbes, X. Jing and L. Zhang, *J. Eng. Fibers Fabr.*, 2021, **16**, DOI: 10.1177/15589250211046242.
20 T. M. Abdelghany, A. M. H. Al-Rajhi, M. A. Al Abboud, M. M. Alawlaqi, A. Ganash Magdah, E. A. M. Helmy and A. S. Mabrouk, *BioNanoScience*, 2018, **8**, 5–16.
21 A. Gour and N. K. Jain, *Artif. Cell Nanomed. Biotechnol.*, 2019, **47**, 844–851.
22 M. G. Sethuraman and N. Sulochana, *Curr. Sci.*, 1986, **55**, 343.
23 P. Yasotha, V. Kalaiselvi, N. Vidhya, V. Ramya and D. P. Srivatsav, *Int. J. Adv. Eng. Sci.*, 2020, **2020**, 1584–1588.
24 T. Parandhaman, M. D. Dey and S. K. Das, *Green Chem.*, 2019, **21**, 5469–5500.
25 T. Li and S. Takkellapati, *Biofuel Bioprod. Biorefining*, 2018, **12**, 756–787.
26 S. Singh, J. V Gade, D. K. Verma, B. Elyor and B. Jain, *Opt. Mater.*, 2024, **152**, 115422.
27 E. L. Irede, R. F. Awoyemi, B. Owolabi, O. R. Aworinde, R. O. Kajola, A. Hazeez, A. A. Raji, L. O. Ganiyu, C. O. Onukwuli and A. P. Onivefu, *RSC Adv.*, 2024, **14**, 20992–21034.
28 S. Fakhari, M. Jamzad and H. Kabiri Fard, *Green Chem. Lett. Rev.*, 2019, **12**, 19–24.
29 E. M. Wong and P. C. Searson, *Appl. Phys. Lett.*, 1999, **74**, 2939–2941.
30 L. Brus, *J. Phys. Chem. Lett.*, 1986, **90**, 2555–2560.
31 N. Ghobadi, *Int. Nano Lett.*, 2013, **3**, 2.
32 J. H. Jun, H. Seong, K. Cho, B.-M. Moon and S. Kim, *Ceram. Int.*, 2009, **35**, 2797–2801.
33 S. Kathirvelu, L. D'souza and B. Dhurai, *Indian J. Fiber Textil Res.*, 2009, **34**, 267–273.

34 T. Tsuzuki, R. He, J. Wang, L. Sun, X. Wang and R. Hocking, *Int. J. Nanotechnol.*, 2012, **9**, 1017–1029.
35 K. Ghule, A. V. Ghule, B.-J. Chen and Y.-C. Ling, *Green Chem.*, 2006, **8**, 1034–1041.
36 R. A. Yuwono, M. F. Izdiharruddin and R. A. Wahyuono, in *Second International Seminar on Photonics, Optics, and Its Applications (ISPhOA 2016)*, SPIE, 2016, vol. 10150, pp. 148–153.
37 I. Chauhan, S. Aggrawal and P. Mohanty, *Environ. Sci.: Nano*, 2015, **2**, 273–279.
38 V. T. Salunke, P. B. Buchade, A. D. Shaligram and R. Y. Borse, *World J. Adv. Res. Rev.*, 2021, **10**, 277–280.
39 T. Fiore and C. Pellerito, *Spectroscopy for Materials Characterization*, 2021, 129–167.
40 A. Ricci, K. J. Olejar, G. P. Parpinello, P. A. Kilmartin and A. Versari, *Appl. Spectrosc. Rev.*, 2015, **50**, 407–442.
41 S. Pasieczna-Patkowska, M. Cichy and J. Flieger, *Molecules*, 2025, **30**, 684.
42 R. Singh and V. D. Mendhulkar, *J. Chem. Pharm. Res*, 2015, **7**, 205–211.
43 P. K. Labhane, V. R. Huse, L. B. Patle, A. L. Chaudhari and G. H. Sonawane, *J. Chem. Eng. Mater. Sci.*, 2015, **3**, 39–51.
44 M. Jia, X. Zhang, J. Weng, J. Zhang and M. Zhang, *J. Cult. Herit.*, 2019, **38**, 64–74.
45 D. S. Corrigan and M. J. Weaver, *J. Phys. Chem. Lett.*, 1986, **90**, 5300–5306.
46 S. Prati, E. Joseph, G. Sciutto and R. Mazzeo, *Accounts Chem. Res.*, 2010, **43**, 792–801.
47 B. Wang, N. Han, D. Meng, R. Yue, J. Yan and Y. Chen, *Particuology*, 2011, **9**, 253–259.
48 R. Hong, T. Pan, J. Qian and H. Li, *Chem. Eng. J.*, 2006, **119**, 71–81.
49 K. Dai, G. Zhu, Z. Liu, Q. Liu, Z. Chen and L. Lu, *Mater. Lett.*, 2012, **67**, 193–195.
50 M. Salavati-Niasari, M. Gholami-Daghian, M. Esmaeili-Zare and F. S. Sangsefidi, *J. Cluster Sci.*, 2013, **24**, 1093–1101.
51 A. D. Khalaji, *Chem. Methodol.*, 2019, **3**, 571–579.
52 C. F. Holder and R. E. Schaak, *ACS Nano*, 2019, **13**, 7359–7365.
53 B. Sun, H. Yu, Y. Yang, H. Li, C. Zhai, D.-J. Qian and M. Chen, *Phys. Chem. Chem. Phys.*, 2017, **19**, 26072–26084.
54 R. Sathyavathi, M. B. Krishna, S. V. Rao, R. Saritha and D. N. Rao, *Adv. Sci. Lett.*, 2010, **3**, 138–143.
55 M. Imath, J. Giri, F. Mohammad and C. Ragavendran, *Microb. Pathog.*, 2025, **199**, 107139.
56 C. Ragavendran, C. Kamaraj, K. Jothimani, A. Priyadharsan, D. A. Kumar, D. Natarajan and G. Malafaia, *Sustain. Mater. Technol.*, 2023, **36**, e00597.
57 R. P Singh, V. K Shukla, R. S Yadav, P. K Sharma, P. K Singh and A. C Pandey, *Adv. Mater. Lett.*, 2011, **2**, 313–317.
58 S. Mourdikoudis, M. Menelaou, N. Fiuza-Maneiro, G. Zheng, S. Wei, J. Pérez-Juste, L. Polavarapu and Z. Sofer, *Nanoscale Horiz.*, 2022, **7**, 941–1015.
59 R. Mohammadinejad, S. Karimi, S. Iravani and R. S. Varma, *Green Chem.*, 2016, **18**, 20–52.
60 S. Balta, A. Sotto, P. Luis, L. Benea, B. Van der Bruggen and J. Kim, *J. Membr. Sci.*, 2012, **389**, 155–161.
61 M. Saeed, H. M. Marwani, U. Shahzad, A. M. Asiri and M. M. Rahman, *Chem. Rec.*, 2024, **24**, e202300106.
62 S. Raha and M. Ahmaruzzaman, *Nanoscale Adv.*, 2022, **4**, 1868–1925.
63 D. P. Sagar Raut and R. Thorat, *Int. J. Sci. Res*, 2015, **4**, 1225–1228.
64 G. Madhumitha, G. Elango and S. M. Roopan, *Appl. Microbiol. Biotechnol.*, 2016, **100**, 571–581.
65 D. L. Aulifa, B. Amarilis, L. N. Ichsani, D. S. Maharani, A. M. Shabrina, H. Hanifah, R. P. Wulandari, A. Rusdin, L. Subra and A. Budiman, *Pharmaceuticals*, 2024, **17**, 1684.
66 M. Abdel-Rahman, H. Ibrahim, M. Y. A. Mostafa, M. A. Abdel-Rahman, M. R. Ebied and E. A. Badawi, *Phys. Scr.*, 2021, **96**, 95704.
67 R. Lal, T. Gour, N. Dave, N. Singh, J. Yadav, A. Khan, A. Jain, L. K. Agarwal, Y. K. Sharma and K. Sharma, *Front. Chem.*, 2024, **12**, 1370667.
68 M. A. Ismail, K. K. Taha, A. Modwi and L. Khezami, *J. Ovonic Res*, 2018, **14**, 381–393.
69 A. C. Janaki, E. Sailatha and S. Gunasekaran, *Spectrochim. Acta, Part A*, 2015, **144**, 17–22.
70 N. Rajabairavi, C. S. Raju, C. Karthikeyan, K. Varutharaju, S. Nethaji, A. S. H. Hameed and A. Shajahan, in *Recent Trends in Materials Science and Applications: Nanomaterials, Crystal Growth, Thin Films, Quantum Dots, & Spectroscopy (Proceedings ICRTMSA 2016)*, Springer, 2017, pp. 245–254.
71 K. Rambabu, G. Bharath, F. Banat and P. L. Show, *J. Hazard Mater.*, 2021, **402**, 123560.
72 A. K. Mandal, S. Katuwal, F. Tettey, A. Gupta, S. Bhattarai, S. Jaisi, D. P. Bhandari, A. K. Shah, N. Bhattarai and N. Parajuli, *Nanomaterials*, 2022, **12**, 3066.
73 T. Dayakar, K. V. Rao, K. Bikshalu, V. Rajendar and S.-H. Park, *Mater. Sci. Eng. C*, 2017, **75**, 1472–1479.
74 M. Patel, S. Mishra, R. Verma and D. Shikha, *Discov. Mater.*, 2022, **2**, 1.
75 D. E. Djeussi, J. A. K. Noumedem, J. A. Seukep, A. G. Fankam, I. K. Voukeng, S. B. Tankeo, A. H. L. Nkuete and V. Kuete, *BMC Compl. Alternative Med.*, 2013, **13**, 1–8.
76 P. Ngamsurach and P. Praipipat, *RSC Adv.*, 2022, **12**, 26435–26454.
77 A. W. Bauer, D. M. PERRY and W. M. M. KIRBY, *AMA archives of internal medicine*, 1959, **104**, 208–216.
78 Y. Zhan, H. Hu, Y. Yu, C. Chen, J. Zhang, K. V. Jarnda and P. Ding, *J. Biomed. Mater. Res.*, 2024, **112**, 1343–1363.
79 P. Parvekar, J. Palaskar, S. Metgud, R. Maria and S. Dutta, *Biomater. Invest. Dent.*, 2020, **7**, 105–109.